Evidence of oxygen vacancy enhanced room-temperature ferromagnetism in Co-doped ZnO

H. S. Hsu and J. C. A. Huang[a)]
Department of Physics, National Cheng Kung University, Tainan 701, Taiwan, Republic of China, Department of Applied Physics, National University of Kaohsiung, Kaohsiung 811, Taiwan, Republic of China, and Center for Micro/Nano Technology Research, National Cheng Kung University, Tainan 701, Taiwan, Republic of China

Y. H. Huang, Y. F. Liao, M. Z. Lin, and C. H. Lee
Department of Engineering and System Science, National Tsing-Hua University, Hsinchu 30013, Taiwan, Republic of China

J. F. Lee
National Synchrotron Radiation Research Center, Hsinchu 30076, Taiwan, Republic of China

S. F. Chen, L. Y. Lai, and C. P. Liu
Department of Materials Science and Engineering, National Cheng Kung University, Tainan 701, Taiwan, Republic of China

(Received 9 December 2005; accepted 1 May 2006; published online 16 June 2006)

The annealing effects on structure and magnetism for Co-doped ZnO films under air, Ar, and Ar/H_2 atmospheres at 250 °C have been systematically investigated. Room-temperature ferromagnetism has been observed for the as-deposited and annealed films. However, the saturation magnetization (M_s) varied drastically for different annealing processes with $M_s \sim 0.5$, 0.2, 0.9, and 1.5 μ_B/Co for the as-deposited, air-annealed, Ar-annealed, and Ar/H_2-annealed films, respectively. The x-ray absorption spectra indicate all these samples show good diluted magnetic semiconductor structures. By comparison of the x-ray near edge spectra with the simulation on Zn *K* edge, an additional preedge peak appears due likely to the formation of oxygen vacancies. The results show that enhancement (suppression) of ferromagnetism is strongly correlated with the increase (decrease) of oxygen vacancies in ZnO. The upper limit of the oxygen vacancy density of the Ar/H_2-annealed film can be estimated by simulation to be about 1×10^{21} cm^{-3}. © *2006 American Institute of Physics*. [DOI: 10.1063/1.2212277]

Transition metal (TM)-doped oxides have been investigated as a promising class of diluted magnetic semiconductors (DMSs) to bring out advanced spintronic devices since the discovery of room-temperature (RT) ferromagnetism in these systems. However, a number of studies[1] indicate that the RT ferromagnetism in TM-doped oxides may come from precipitation of magnetic clusters or from secondary magnetic phases. On the other hand, there are reports that suggest the absence of magnetic clusters or secondary phases and support intrinsic ferromagnetic origin.[2] Even so, the origin of ferromagnetism in oxide DMSs remains a very controversial topic. For example, a carrier-mediated mechanism has been proposed to explain the ferromagnetism in oxide DMSs. However, the TM-doped oxide films with ferromagnetic properties are sometimes poor in conducting or even highly insulating.[3,4] The *sp-d* exchange mechanism between the *sp* free carriers and the *d* states of the TM doping elements is therefore inapplicable in these cases. Double exchange mechanism between *d* states of TM elements is another possible candidate to induce ferromagnetism in magnetic oxide. However, in many cases the low doping concentration and single valence state of magnetic elements have been observed to exclude the double exchange mechanism.

In addition to the magnetic doping effect, oxygen vacancies have been proposed to play an important role in the magnetic origin for oxide DMSs. For example, theoretical studies suggest that oxygen vacancies can cause a marked change of the band structure of host oxides and make a significant contribution to the ferromagnetism.[5,6] The formation of bound magnetic polarons (BMPs), which include electrons locally trapped by oxygen vacancies, with the trapped electron occupying an orbital overlapping with the *d* shells of TM neighbors, has also been proposed to explain the origin of RT ferromagnetism for some insulating oxide DMSs.[7] Experimentally, oxygen vacancies might easily be generated during various thin film growth processes owing to the vacuum environments. Many controversial results of oxide DMSs could possibly be related to the variation of their oxygen vacancies.[8,9] However, oxygen vacancies are difficult to measure. In this letter, we study the correlation of electronic structure, local structure, and magnetic properties of Co-doped ZnO thin films. We show that x-ray near edge spectroscopy (XANES) on Zn *K* edge is sensitive to the formation of oxygen vacancies in ZnO modulated by annealing processes. The change in preedge feature of XANES spectra is likely associated with the concentration variation of oxygen vacancy as revealed by the scattering calculation. Evidence of oxygen vacancy enhanced magnetization is provided by comparison of the magnetic and XANES results.

Several Co-doped ZnO films of about 550 Å were simultaneously grown on α-Al_2O_3 (0001) substrates at RT by ion beam sputtering using a multilayer doping technique. Details of similar sample preparation procedures have been described elsewhere.[10] After the growth, these films were separately annealed under air, 1 atm of pure Ar, and 1 atm of

a)Electronic mail: jcahuang@mail.ncku.edu.tw

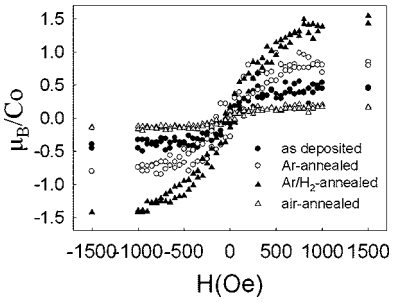

FIG. 1. (Color online) The magnetization vs magnetic field curves for the as-deposited and annealed Co:ZnO films measured at room temperature.

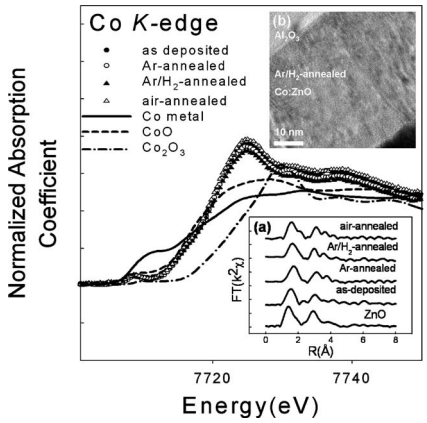

FIG. 2. (Color online) The Co *K*-edge XANES for the as-deposited sample and annealed films. The XANES of Co foil and Co oxides are also provided for reference. Inset (a) shows the FT amplitudes of Co *K*-edge EXAFS for the as-deposited and annealed films together with the Zn *K* edge of ZnO (500 Å) for reference. Inset (b) shows the HRTEM image for the Ar/H_2-annealed sample.

$Ar(90\%)/H_2(10\%)$, each at 250 °C for 1 h, respectively. Samples studied here are all textured films with the *c* axis directed out of the plane, as evidenced by x-ray diffraction. The Co to Zn ratio extracted from the energy dispersive x-ray (EDX) spectra is about $6\pm1\%$.

The magnetic properties of these samples were performed by a commercial superconducting quantum interface device (SQUID). RT ferromagnetism has been observed for the as-deposited and annealed films, as shown in Fig. 1. For this series of films, the Ar-annealed and Ar/H_2-annealed films show saturation magnetization (M_s) of about 0.9 and 1.5 μ_B/Co, respectively, the latter about triple of the as-deposited film (0.5 μ_B/Co). On the other hand, the M_s of the air-annealed film (0.2 μ_B/Co) is less than half of the as-deposited film. Similar annealing effect on magnetism for oxide DMSs has also been reported by other research groups.[8,9] However, in some cases the enhanced ferromagnetism may come from the precipitation of magnetic clusters.[11] Therefore, it is essential to realize the annealing effect on the local structure in the first place in order to disclose the origin of ferromagnetism in oxide DMSs.

The x-ray absorption spectroscopy (XAS) technique has been demonstrated as a powerful tool to understand the local structure of DMSs.[1,10] The XAS experiments were carried out in the wiggler-C beamline of the Taiwan Light Source in Hsinchu, Taiwan. XANES is a fingerprint of the electronic state (particularly of the valence state) of TM elements, and is extremely sensitive to inspect the presence of Co clusters in host oxides.[12] The XANES spectra on Co *K* edge of the as-deposited, air-, Ar-, and Ar/H_2-annealed Co:ZnO samples are displayed in Fig. 2. XANES from a standard Co foil and CoO and Co_2O_3 powders are also provided as reference. It is noticed that the preedge feature for the as-deposited and annealed samples resembles much as the CoO reference, in marked contrast with the characteristic of metallic Co with a significant shoulder around 7712 eV. The XANES measurements revel that most of the Co atoms in all of these samples are in the +2 state. Besides, extended x-ray absorption fine structure (EXAFS) spectra on Co *K* edge of these films have been used to clarify the local structures surrounding Co. Inset (a) of Fig. 2 shows the Fourier transform (FT) amplitude of EXAFS on Co *K* edge for these samples, together with the Zn *K* edge of ZnO film (500 Å) as reference. For the as-deposited and annealed Co:ZnO samples, the Co *K* edge FT spectra are very similar to the undoped ZnO film as viewed from a specific Zn atom. The results reveal that most of the Co atoms substitute for Zn atoms for all the Co:ZnO samples studied here.

The magnetic and XAS results suggest that the observed RT ferromagnetism for the as-deposited and annealed samples is in accordance with Co cluster-free structures, which is consistent with the high resolution transmission electron microscopy (HRTEM) results shown, for example, in the inset (b) of Fig. 2. Note that if the ferromagnetic signal, for example, in the Ar/H_2-annealed sample, were due to precipitation of Co clusters, the measured moment of 1.5 μ_B/Co indicates that about 90% of the Co atoms exists in the form of metallic Co clusters (1.7 μ_B/Co for bulk Co), and such a high concentration of metallic Co clusters would be easily detected by XAS or TEM.

In addition, the RT resistivity of the Ar/H_2-annealed sample ($\sim 2\times10^{-2}$ Ω cm) is lower than the Ar-annealed sample ($\sim 6\times10^{-2}$ Ω cm) and the as-deposited one ($\sim 7\times10^{-1}$ Ω cm). The resistivity trend seems to support the model of carrier-mediated ferromagnetism. However, the air-annealed film is highly insulating ($\sim 6\times10^{3}$ Ω cm), yet it still displays robust ferromagnetism. This case makes carrier-mediated mechanism invalid.

Our systematic studies show that oxygen vacancy constituted BMPs are a promising candidate for the origin of RT ferromagnetism in this system. Within the BMP model, the greater density of oxygen vacancies yields a greater overall volume occupied by BMPs, thus increasing their probability of overlapping more Co ions into the ferromagnetic domains and enhancing ferromagnetism.[7] To further probe the role of the oxygen vacancies on magnetic behavior, we therefore carry out the XANES measurements on Zn *K* edge. In contrast with the similar Co *K*-edge results for the as-deposited and annealed Co:ZnO samples, the Zn *K*-edge results of these samples show some variation in the preedge region. Figure 3 presents the Zn *K*-edge XANES spectra for the ZnO film, the as-deposited, and the annealed Co:ZnO samples. The characteristic peaks "A" and "B" were observed for all of these films and can be referred to as the Zn 1*s*-4*p* transitions. The integrated area of the Zn *K*-edge XANES spectra, which is proportional to the unfilled *p* density of states (DOSs) in Zn, is much smaller for the as-deposited and Ar- and Ar/H_2-annealed samples compared with the air-annealed sample; the latter is almost equivalent to the ZnO film. This means that either the moderate doping or annealing processes increase the carriers, and therefore, decrease the unfilled *p* DOSs. But for the air-annealed sample, the annealing

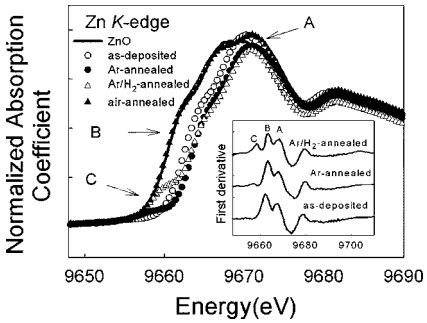

FIG. 3. (Color online) The Zn *K*-edge XANES for the ZnO (500 Å), as-deposited, and annealed films. The inset shows the first derivative of XANES for these films.

process causes oxygen to rediffuse into the film, thus removing the oxygen vacancies and increasing the unfilled *p* DOSs. These results are consistent with the electrical measurements mentioned above. Besides, it is noticed that an additional preedge peak labeled "C" can be observed in the XANES spectra for the Ar- and Ar/H_2-annealed samples and it becomes more manifest in its first derivative, as shown in the inset of Fig. 3. Note that the intensity of the preedge peak C is much pronounced for the Ar/H_2-annealed sample. In general, the preedge feature is a characteristic only for TM due to $1s$-$3d$ transitions, such as for Co discussed above. For ZnO with a completely filled $3d$ orbital (i.e., Zn $3d^{10}$), the preedge peak can be considered as defect-induced local interference effect around the Zn absorber rather than bound state transitions.[13]

To verify the influence of Co substitution for Zn and the formation of oxygen (O) vacancies on the preedge feature, we carry out the XANES simulation taking account of several structural variants. The modeled spectra were calculated by the real-space multiple-scattering approach using FEFF 8.2 code[14] operating on Zn *K* edge. The scattering potentials were calculated self-consistently in a cell cluster of 27 atoms (up to three coordination shells). Hedin-Lundquist exchange correlation potential was used in this simulation. The FEFF input file was generated by the ATOMS package for the lattice constants $a=3.249$ Å and $c=5.206$ Å. As shown in Fig. 4(a), the calculated spectra for a cell cluster with three coordination shells are already in reasonably good agreement with the experimental curves and reproduce the main features (A_1 and B_1). It is also noted that the increase of more coordination shells does not lead to significant change in the line shape of the simulated spectra. For clarity, the derivative XANES spectra are provided in Fig. 4(b).

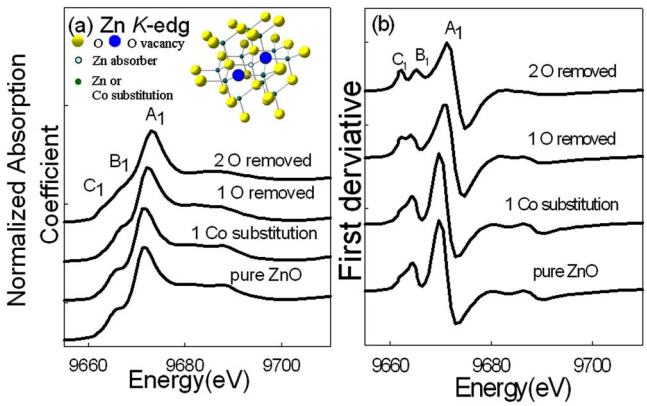

FIG. 4. (Color online) Theoretical XANES (a) and their first derivative (b) on Zn *K* edge from FEFF simulation for a ZnO cell cluster (27 atoms) and several structural variants, including the influence of Co substitution and oxygen vacancies.

For the case of one Co substitution (~6% Co doping), the simulated XANES results on Zn *K* edge resemble much of that of a pure ZnO due to similar photoelectron scattering function for Co and Zn in the studied energy region.[15] For the case of O vacancies, on the other hand, the simulation results indicate that Zn *K*-edge XANES shows some variation from a pure ZnO. This is reasonable because low atomic number (Z) element such as oxygen has stronger scattering factor in the XANES energy region. For example, by removing one of the O atoms in the first coordination, an additional preedge peak "C_1" appears, as shown in Fig. 4. By removing two O atoms (one in the first and another in the second coordination shell of O, for example), the C_1 peak intensity becomes more pronounced.

The amount of oxygen vacancies among these DMS films can be qualitatively understood by comparison of the experimental (Fig. 3) and theoretical (Fig. 4) XANES spectra on Zn *K* edge. The Ar/H_2-annealed film with the most pronounced preedge peak possesses more oxygen vacancies than the Ar-annealed and as-deposited samples. Oxygen vacancies are largely reduced for the air-annealed film. Within the simulation model, the upper limit of the density of oxygen vacancies (of the Ar/H_2-annealed film) can be estimated to be about 1×10^{21} cm^{-3}. More quantitative analysis of the oxygen vacancies in Co:ZnO film are under intensive studies. We conclude that the variation of oxygen vacancies in Co:ZnO is strongly correlated with observed RT ferromagnetism.

This work has been supported by the National Science Council of the ROC under Grant No. NSC 94-2120-M-006-008.

[1]Jung H. Park, Min G. Kim, Hyun M. Jang, Sangwoo Ryu, and Young M. Kim, Appl. Phys. Lett. **84**, 1338 (2004).
[2]S. Ramachandran, Ashutosh Tiwari, and J. Narayan, Appl. Phys. Lett. **84**, 5255 (2004).
[3]K. A. Griffin, A. B. Pakhomov, C. M. Wang, S. M. Heald, and Kannan M. Krishnan, Phys. Rev. Lett. **94**, 157204 (2005).
[4]Zhigang Yin, Nuofu Chen, Chunlin Chai, and Fei Yang, J. Appl. Phys. **96**, 5093 (2004).
[5]John E. Jaffe, Timothy C. Droubay, and Scott A. Chambers, J. Appl. Phys. **97**, 073908 (2005).
[6]Hongming Weng, Xiaoping Yang, Jinming Dong, H. Mizuseki, M. Kawasaki, and Y. Kawazoe, Phys. Rev. B **69**, 125219 (2004).
[7]J. M. D. Coey, M. Venkatesan, and C. B. Fitzgerald, Nat. Mater. **4**, 173 (2005).
[8]Nguyen Hoa Hong, Joe Sakai, Ngo Thu Huong, Nathalie Poirot, and Antoine Ruyter, Phys. Rev. B **72**, 045336 (2005).
[9]A. Manivannan, G. Glaspell, P. Dutta, and M. S. Seehra, J. Appl. Phys. **97**, 10D325 (2005).
[10]J. C. A. Huang, H. S. Hsu, Y. M. Hu, C. H. Lee, Y. H. Huang, and M. Z. Lin, Appl. Phys. Lett. **85**, 3815 (2004).
[11]0.D. H. Kim, J. S. Yang, Y. S. Kim, T. W. Noh, S. D. Bu, S. I. Baik, Y. W. Kim, Y. D. Park, S. J. Pearton, J. Y. Kim, J. H. Park, H. J. Lin, C. T. Chen, and Y. J. Song, Phys. Rev. B **71**, 014440 (2005).
[12]T. C. Kaspar, T. Droubay, C. M. Wang, S. M. Heald, A. S. Lea, and S. A. Chambers, J. Appl. Phys. **97**, 073511 (2005).
[13]David A. McKeown, Phys. Rev. B **45**, 2648 (1992).
[14]A. L. Ankundinov, B. Ravel, J. J. Rehr, and S. D. Conradson, Phys. Rev. B **58**, 756 (1998).
[15]*Handbook of Synchrotron Radiation*, edited by E. A. Stern, S. M. Heald, and E. E. Koch (North-Holland, New York, 1983), pp. 995–1014.